Available online at www.sciencedirect.com
SCIENCE DIRECT®
Engineering Geology 70 (2003) 109–130
ENGINEERING GEOLOGY
www.elsevier.com/locate/enggeo

Instability conditions of marly hillslopes: towards landsliding or gullying? The case of the Barcelonnette Basin, South East France

O. Maquaire[a], J.-P. Malet[a,*], A. Remaître[a], J. Locat[b], S. Klotz[c], J. Guillon[c]

[a] *Institut de Physique du Globe, UMR 7516 CNRS-ULP, EOST, 5, rue René Descartes, F-67084 Strasbourg, France*
[b] *Département de Géologie et Génie Géologique, Université Laval, Sainte-Foy, Québec, Canada G1K 7P4*
[c] *Faculté de Géographie et d'Aménagement, 3, rue de l'Argonne, F-67083 Strasbourg, Cedex, France*

Received 29 July 2002; accepted 6 March 2003

Abstract

Black marl hillslopes in the French Alps are strongly affected either by mass movements or by gully erosion due to their susceptibility to weathering processes. This paper presents experimental data (geomorphological, geotechnical, geomechanical and hydrological) on the parameters of the material of three well-known earthflows and of the two stratigraphic parts of the Callovo–Oxfordian black marl. The main objectives are to define the geomechanical behaviour of the various formations using different characterisations (grain size distribution, mineralogy, retention capacity, consolidation test, direct shear test and triaxial test) and to demonstrate how such soils can affect the stability of natural slopes. Particular care must be taken when interpreting the geomechanical tests on this evolving and very heterogeneous clay-rich material. There are strong relationships between the parent rock and the landslide materials. This paper presents a conceptual model of the development of strength over a period of time and investigates the parameters of the material for use in slope stability analysis and risk assessment.

Keywords: Black marl; Landslides; Soil parameters; Strength; Weathering; South East France

1. Introduction

The Southeastern part of the French Alps is made up of sedimentary rocks comprising alternating marl and limestone sequences whose ages range from Lias to Cretaceous. The oldest marly sequence, called ''Terres Noires'' (Bathonian to Oxfordian), is delimited in the West by the Rhône valley, in the North by the latitude of Grenoble, in the East by the Italian border and in the South by the Provence Prealps (Fig. 1a).

Large-scale slope failures and extended gullied areas (badlands) are significant processes in these black marl deposits; they represent a high risk to the neighbouring population because of the considerable volume and the potential speed of slide-induced-debris-flows. The volumes range from tens of cubic metres to over 1 million and the velocity of debris-flows can easily exceed 3–5 m s^{-1} (Malet et al., 2002b; Remaître et al., 2002). Both small and large failures have been

* Corresponding author. Fax: +33-3-9024-0900.
E-mail address: jeanphilippe.malet@eost.u-strasbg.fr (J.-P. Malet).

0013-7952/03/$ - see front matter © 2003 Elsevier Science B.V. All rights reserved.
doi:10.1016/S0013-7952(03)00086-3

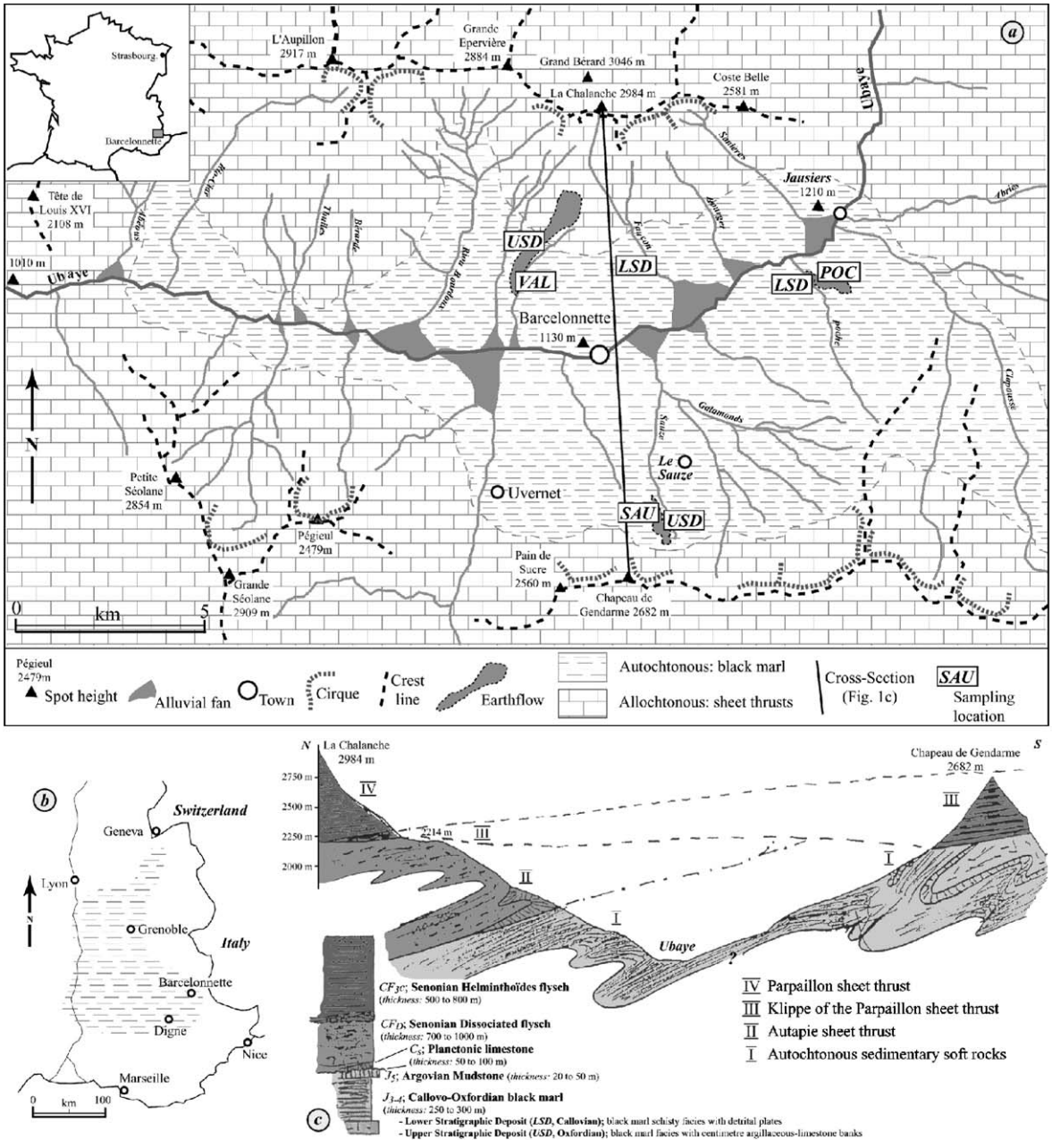

Fig. 1. (a) Extent of the black marl formation in France; (b) simplified geomorphological sketch of the Barcelonnette Basin; (c) geological cross-section of the Barcelonnette Basin (after Flageolet, unpublished).

observed in this formation, in the Baronnies (Chodzco et al., 1991; Garnier and Lecompte, 1996), in the Buëch region (Olivry and Hoorelbeck, 1989), in the Digne region (Oostwoud Wijdenes and Ergenzinger, 1998) and especially in the Barcelonnette Basin (Flageollet et al., 2000; Malet et al., 2000; Maquaire et al., 2001), where three large slope failures have occurred in the 20th century; these have now become earthflows.

Landscapes in the Barcelonnette Basin (Alpes-de-Haute-Provence, France) closely resemble mass-wasting processes and/or badlands. Earlier research on marly landscapes (Gerrits et al., 1987; Imeson and Verstraten, 1988; Maquaire et al., 2002) showed that formations with similar morphological and sedimentological characteristics were affected differently by mass-wasting processes and by rill erosion. Mass-wasting was often found to be prevalent in more cohesive soils because of their higher retention capacity, whereas gully erosion is commonly observed on more silty soils (Martínez-Mena et al., 2002). These differences in the dominant geomorphological processes coincided with differences in a number of hydrological and geotechnical parameters (such as microclimate, vegetation and soil surface characteristics; Malet et al., in press; Harvey and Calvo, 1991). Gravels, sands and clays have received considerable attention in the hydrological and geotechnical literature but there has been much less research into the behaviour of more silty formations, such as the black marl, in spite of the fact that they cover over 10,000 km^2 in southeast France (Légier, 1977; Phan and Antoine, 1994; Antoine et al., 1995). A general lack of awareness of the special nature of this clay-bearing, silty rock, which can swell or disintegrate when exposed to atmospheric triggers (wetting–drying cycles and freeze–thaw cycles), is illustrated by the failure to predict the formation of mudflows, large earthflows and debris-flows due to the complex evolution and alteration of the material under testing procedures (Antoine et al., 1995). The heterogeneity of this material makes mechanical and hydrological characterisation difficult, and specific protocols must be designed to obtain realistic grain size distributions and strength values.

This lack of awareness is also illustrated in several current geotechnical and landslide classification schemes, which fail to recognise silty formations (and therefore marl) as a distinctive category of landslide-prone materials. One consequence of this has been a tendency to regard black marl landslides as "typical", whereas it is now known (Antoine et al., 1988; Maquaire et al., 2001) that mass movements in marl cover a wide range of types.

This paper presents experimental data on the hydrological and geotechnical parameters of the two stratigraphic parts (upper and lower) of the Callovo–Oxfordian black marl in the Barcelonnette Basin and the effect of changing moisture contents on the strength of both "undisturbed" and remoulded samples has proved to be of particular interest. The purpose of this study is thus twofold. Firstly, specific issues (representativeness, heterogeneity, specific protocol) are proposed to define the geomechanical behaviour of the marl overall, on the basis of former studies on black marl characterisation. Secondly, it examines the data obtained from in situ tests and tests in the laboratory. This section analyses the hydrological and geomechanical behaviour of three different earthflows and in situ weathered regolith and assesses the effects of such soil layers on the stability of natural slopes. We observed strong relationships between the parent rock and the landslide material, and we have developed a conceptual model of the evolution of strength over a period of time.

2. Geological and geomorphological background of the Barcelonnette Basin

2.1. The Barcelonnette Basin: lithologic and climatologic factors

The Barcelonnette Basin is a geological window in two Eocene crystalline sheet thrusts (Autapie and Parpaillon) that overlay the black marl (Fig. 1b and c). The thickness of the Jurassic "Terres Noires" reaches 250–300 m. Three subsets can be distinguished: firstly, the Lower Callovian black marl with detrital plates (50–60 m thick); secondly, the Middle and Upper Oxfordian black marl (150–250 m thick), with centimetre argillaceous-limestone banks; and thirdly, some rare outcrops of Argovian black marl (15–20 m thick). The extent of the Callovian and the Oxfordian deposits (BRGM, 1974; Fig. 1b and c) cannot be mapped separately because of the morainic cover.

The Callovian black marl (Lower Stratigraphic Deposit, LSD) presents grey clayey schist facies, very finely laminated, with a few argillaceous-limestone beds. The Oxfordian black marl (Upper Stratigraphic Deposit, USD) presents more calcareous black facies, less laminated (Artru, 1972; Awongo, 1984; Phan, 1993). Their susceptibility to mass movements can be

partly accounted for by microtectonics, forming potential sliding surfaces and guiding fragmentation and weathering. The morphology of the clasts depends on the orientation of the bedding joints, the schistosity and the carbonate content of the marl (Coulmeau, 1987; Alexandre, 1995).

The Barcelonnette Basin has a dry and mountainous Mediterranean climate with a strong interannual rainfall variability (733 ± 412 mm over the period 1928–2002), strong storm intensities (over 50 mm h^{-1}) and 130 days of freezing per year. These characteristics imply significant daily thermal amplitudes and a great number of freeze–thaw cycles.

2.2. Landslides and badlands characteristics in the "Terres Noires" of the Barcelonnette basin

The morphological development of the marly slopes by gullying or mass-movements is supported by the conjunction of these lithologic and climatic factors, (Flageollet et al., 1996, 1999). Summer storms give rise to Hortonian runoffs with a strong erosive capacity after long dry periods which form very thick surface crusts (Descroix and Olivry, 2002). In spring, the marl is soaked by snow melting and undergoes another type of erosion by pellicular solifluction. The characteristics of the rock mass may also trigger rock block slides (Malet et al., 2000) and the accumulated material can evolve into channelised earthflows (Poche POC, Super-Sauze SAU, La Valette VAL). Geomorphological forms developed in the "Terres Noires" thus comprise very steep (>65%) naked badlands areas (Fig. 2a) and very heterogeneous accumulation zones (Fig. 2b–d). The soil surface conditions in these areas are very heterogeneous and directly controlled by the particular weathering of the rock (Malet et al., in press).

Landslides occur mainly in the upper slopes in the Upper Stratigraphic Deposit (USD), while gullying occurs mainly in the lowest slopes in the Lower Stratigraphic Deposit (LSD), though occasional slumps and streambanks failures can be located in it. This implies that these two morphological processes are potentially governed by the sedimentological, mineralogical, hydrological and geotechnical characteristics of the stratigraphic deposits.

2.3. The study areas: the Poche, Super-Sauze and La Valette earthflows

The gullied areas apart, the Barcelonnette Basin is characterised by three earthflows. The Poche earthflow (Fig. 2d) is the only landslide developed in the LSD; it lies between 1239 and 1502 m of elevation and has been less active since the beginning of the 19th century. The volume is 600,000–700,000 m^3 (Guillon, 2001). The topography of the ablation zone is chaotic, with marly panels, moraine deposits and sides of herbaceous and forest vegetation. The bordering torrent soaks the accumulated material and thus contributes to the initiation of very fluid debris-flows. The most significant can reach the Ubaye River, as in 1957 (Lecarpentier, 1963). The earthflow has an average velocity of less than 0.01 m day^{-1}.

The Super-Sauze earthflow has developed in an enclosed torrential watershed in the USD. Its elevation is between 2105 m (crown) and 1740 m (toe of the flow) with a 25° slope, over a 17-ha area (Fig. 2c). There were block falls and structural slides of large slabs in the 1960s and the flow developed through the 1970s, burying a stream channel. The paleotopography, a succession of more or less parallel crests and gullies, plays an essential role in the behaviour of the flow by delimiting preferential water and material pathways and compartments with differing kinematical, mechanical and hydrological characteristics (Maquaire et al., 2001). The total volume is estimated at 750,000 m^3 and velocities range from 0.01 to 0.4 m day^{-1}. Three debris-flows were triggered in the upper part of the flow in 1999 and 2000 (Malet et al., submitted for publication, a).

The complex mass-movement of La Valette (Fig. 2b), amounting to a volume of 3,500,00 m^3 of displaced material, originates in a succession of interrelated mass movement events commencing in March 1982. This slide was triggered by the critical pore pressures at the boundary between the underlying impervious USD and the permeable, coarser material of the Autapie sheet thrust (Van Beek and Van Asch, 1996). Catastrophic movements occurred in January 1988, after an abrupt thaw, where pore water pressures forced a flow of over 50,000 m^3 of material. The subsequent stress release in the source area and similar thawing conditions in March 1988 initiated a second debris-flow with a smaller run-out distance.

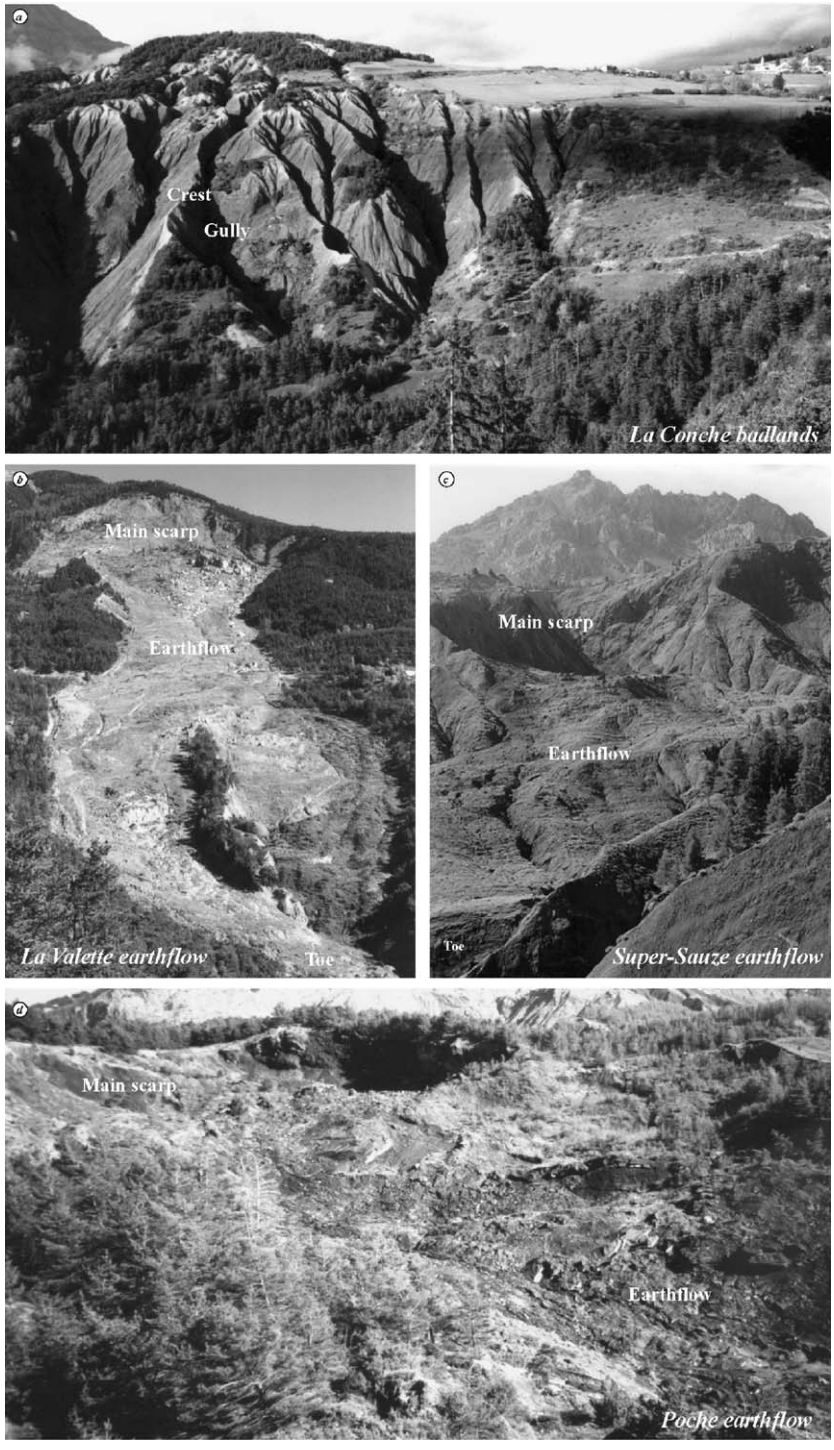

Fig. 2. Specific landscapes developed in the black marl formation. (a) Badland hillslope in LSD, near the village of La Conche; (b) the La Valette (VAL) earthflow at the contact between USD and the Autapie sheet thrust; (c) the Super-Sauze (SAU) earthflow in USD; (d) the upper part of the Poche (POC) earthflow in LSD.

The highest velocities of the earthflow reach 0.2–0.4 m day^{-1}, while the mean velocities are near 0.01 m day^{-1} for Poche and Super-Sauze.

The development of all three earthflows is controlled by the progressive transformation of the geomechanical characteristics of the weathered material and by the increase in pore water pressures, dependent on seasonal fluctuation and events in a free groundwater table located in the subsurface (Malet et al., 2002a). The three earthflows bodies mainly comprise a marly matrix (with a silty–sandy texture) which incorporates marly clasts, pyrite or calcite pieces and morainic stones.

3. Materials and methods

The test program carried out during this work included: (1) analysing the mineralogy using the X-ray diffraction technique, (2) determining the physical parameters of the materials (grain size distribution, carbonate content, bulk and dry densities, methylene blue value and Atterberg limits), (3) analysing the hydrological behaviour of the formations (saturated and unsaturated conductivity and retention capacity), and (4) standard geotechnical tests (consolidation, direct shear, ring shear and triaxial tests). Five types of materials were tested: the superficial reworked part of the three earthflows (VAL, SAU, POC) and the superficial weathered part of the two in situ black marl deposits (USD, LSD). In this study, the in situ weathered part refers to a loosened regolith, where the marl structure has deteriorated; this may be 0.5–1.5 m thick, depending on local structural and topographic conditions (Maquaire et al., 2002). Samples were hand carved in situ (Fig. 1b). Sampling depths were between 0.5 and 1 m. The methods used in this paper were based on the standard protocols described by American Society for Testing and Materials (ASTM) and Association Française de Normalisation (AFNOR). The X-ray diffraction analysis (air dry oriented treatment, glycerol treatment and 500 °C heated treatment) was performed according to Cullity (1989).

4. Parameters of slope-forming materials

4.1. Mineralogy and microstructure of the reworked and weathered black marl formations

The black marls consist of highly stratified rocks, exhibiting a fine bedding inherited from their original deposition by turbidity currents and including a detrital and a carbonated phase. The relatively low carbonate content (essentially calcite) varies from 20% to 35% of the total volume, with corresponding facies ranging from marl to clayey limestone. This low carbonate content explains the formation's high erodibility (Bufalo, 1989). The detrital phase comprises mainly silt (predominantly quartz and feldspaths) with a small proportion of clay materials. No swelling clays (i.e. montmorillonite) are present in the mineralogical spectrum. The low values obtained from methylene blue tests also reveal the absence of swelling clays, with very low quantities of smectite. The tested material shows small variations, and two groups can be distinguished (Fig. 3): firstly, the essentially marly materials (SAU, POC, in situ marl) formed mainly of illites and chlorites and secondly, material which

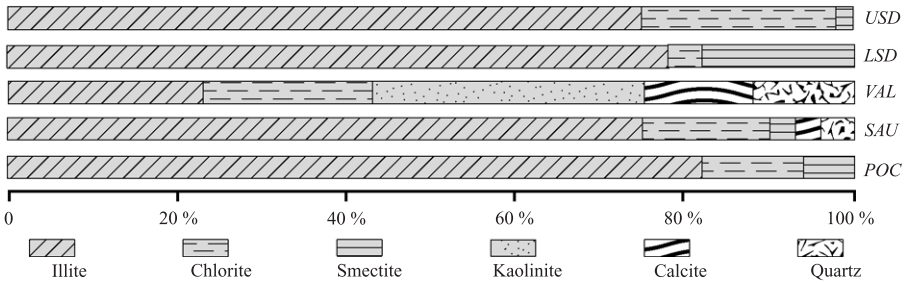

Fig. 3. Mineralogy of the reworked and weathered black marl formations.

corresponds to marl/moraine mixtures (VAL), richer in kaolinite and poorer in illite.

4.2. Physical parameters of the reworked and weathered black marl formations

Physical parameters (Table 1) such as specific gravity, dry unit weight, void ratio and porosity were determined on the undisturbed samples. Bulk unit weight ranges from 12.6 to 17.4 Mg m^{-3} for a specific gravity ρ_s of 2.62–2.71. LSD formation shows a lower bulk density than the USD formation. The natural water content varies considerably, ranging from 8% to 35%; the porosity ranges from 14% to 36% and the void ratio from 0.4 to 2.0. The LSD formation appears less porous than the USD formation.

Results obtained from modified Proctor tests, on the <20 mm fraction, indicate a maximum dry unit weight of 18.1–20.9 kN m^{-3} and an optimum moisture content of 8.9–13.1%. The USD marl may be more fragile during changing moisture conditions and seem more affected by swelling processes, as it is more difficult to produce a compacted soil from this formation, related to a lower carbonate content.

4.3. Grain-size distributions and consistency limits of the reworked and weathered black marl formations

When analysing grain size distribution it is important to note that the heterogeneity of the formations (very fragile marly plates and flakes packed in a fine matrix, and blocks and pebbles of calcite) and the brittleness of the marly clasts require a specific protocol. We analysed the whole granulometric range [0/D_{max}], with a D_{max} fixed at 100–150 mm for the black marl and a significant volume of material must be sampled to obtain representative analyses. This optimal volume (or mass) was ascertained by comparing the clay and silt fractions obtained for various samples masses (weight ranging from 4 to 200 kg, Fig. 4a). The percentage varies from 15% to 57%. The distribution of the values indicates an optimal mass varying from 70 to 110 kg, for a fine fraction content from 33% to 38%. These values are in accordance with those proposed by the Tacnet et al. (2000) empirical rule: $2D$ (mm) < sample mass in kg < $5D$ (mm), which indicates a sample mass of 40–100 kg for the analysis of the fraction 0/20 mm. All the proposed grain size distributions were therefore carried out on a total mass of 100–130 kg.

A cubic hole (20 cm deep) was excavated for each sampling and the samples were air-dried in situ for at least 2 h before weighing. Boulders (>20 mm) sizes were determined in the field. Only a quarter of the matrix sample (<20 mm) was taken for laboratory tests. Samples were sifted through an 18-mesh series (20–0.05 mm) in the laboratory. Finer grain size content (silt and clay) was obtained using a laser diffraction grain-size analyser (Coulter LS-230). All matrix fractions (gravel: >2 mm, sand: 2–0.05 mm, silt: 0.05–0.002 mm, clay: <0.002 mm) are given as percentages by dry mass (Table 2, Fig. 4b).

All matrix samples have a high silt and clay content (from 25% to 40%) and the textural classes range from "silty clay" to "silty sand". The overall particle-size distributions of the five formations are very similar, although the VAL and USD formations are slightly coarser than the other formations. For the three earthflows, the grain size distribution envelopes can be clearly distinguished (defined on four analyses for VAL, five analyses for SAU and five analyses for POC, Fig. 4c). The median diameter (D_{50}) is low and

Table 1
Some physical parameters of the reworked and weathered black marl formations

	Specific gravity	Dry unit weight	Saturated unit weight	Optimum water content	Optimum unit weight of dry soil	Void ratio	Porosity
	ρ_s (Mg m^{-3})	ρ_d (kN m^{-3})	ρ_{sat} (kN m^{-3})	W_{opt} (%)	ρ_{opt} (kN m^{-3})	e dimensionless	n (%)
USD	2.68	14.3–14.7	19.1–19.5	11.5	20.2	0.8–1.0	28–36
LSD	2.62	12.6–12.8	17.1–17.6	9.8	20.9	0.5–0.7	15–19
SAU	2.71	16.6–17.1	20.4–20.7	12.0	19.2	0.5–0.8	23–33
VAL	2.70	13.7–15.1	19.1–20.3	10.6	20.5	0.7–0.8	20–26
POC	2.63	16.9–17.4	20.5–20.9	12.3	18.1	0.5–0.9	17–23

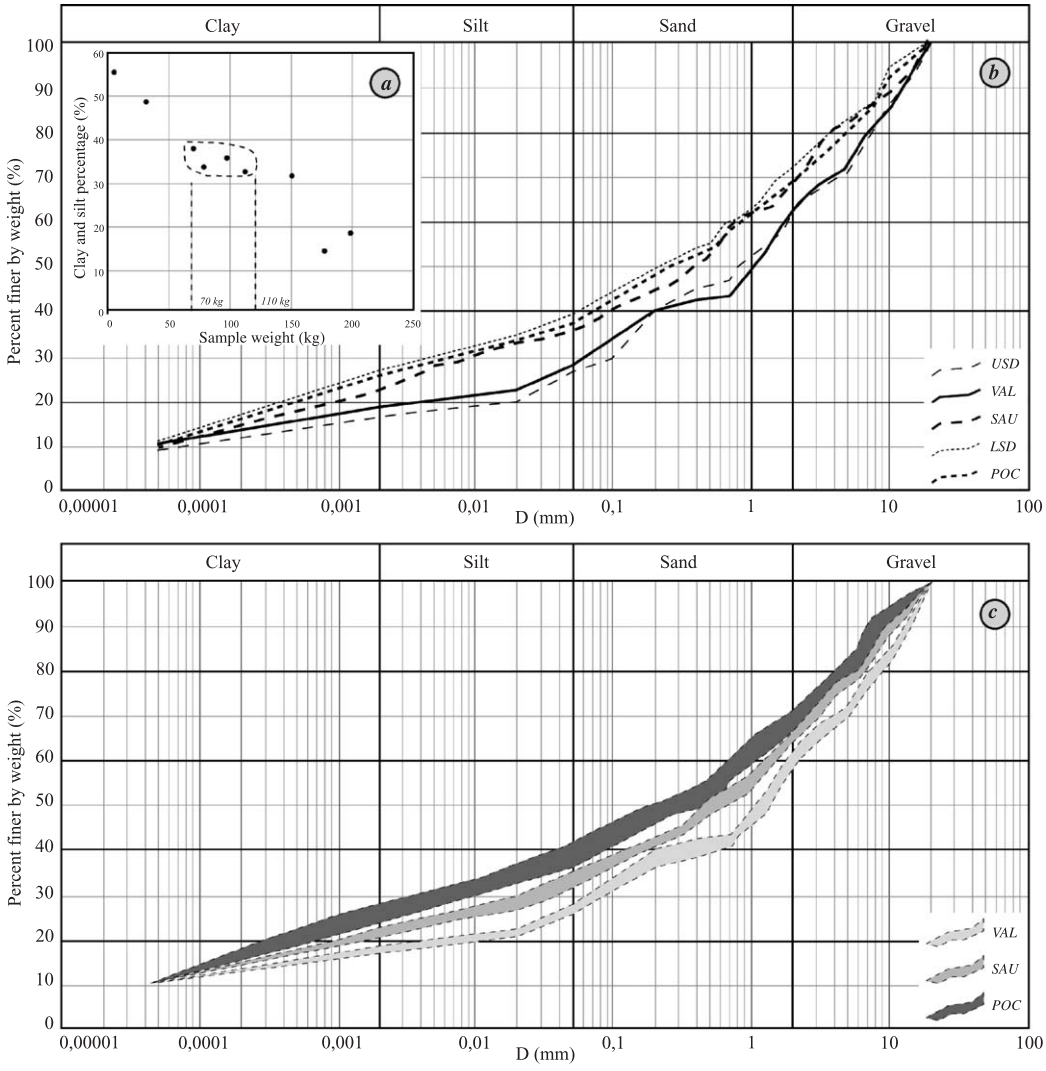

Fig. 4. Grain size distribution fir the various formations. (a) Relationship between the sample mass and the clay percentage; (b) average grain size distribution for the five formations; (c) grain size distribution envelopes defined for the three earthflows.

dispersed (from 0.2 to 0.5 mm) for POC, similar (from 0.4 to 0.5 mm) for SAU and higher (from 1.1 to 1.5 mm) for VAL. These values are related to the age of the earthflows: the clay and silt fraction increases with the age of the earthflow, reaching 36–42% for POC, 32–35% for SAU and 26–27% for VAL. Grain size distributions also show a remarkable correlation between the geological ''source area'' (USD or LSD) and the earthflow formation. For VAL earthflow, the coarser texture can also be related to the Autapie sheet thrust.

Atterberg consistency limits were determined on the silt and clay fraction. Liquid limits were obtained using the percussion method (Casagrande, 1932) and the fall-cone method (Hansbo, 1957). The roller method was used for plastic limits. Atterberg limits (Fig. 5a) classify the LSD formation as inorganic silt of low plasticity ($I_p = 8$ to 9) and the earthflows (SAU, POC, VAL) and the USD formations as inorganic clays of low plasticity ($I_p = 11$ to 19). The liquid limits range from 29% to 38%. The Skempton activity chart (Fig. 5b) illustrates the non-activity of

Table 2
Grain size distribution and consistency indices of the reworked and weathered black marl formations

	Grain size[a]					Atterberg limits					SS[b]	
	Gravel (%)	Sand (%)	Silt (%)	Clay (%)	*n*	W_l (%)	W_p (%)	W_r (%)	I_p	*n*	SS (m^2/g)	*n*
USD	37–39	36–38	8–11	16–17	2	33–35	16–18	14–15	16–18	5	/	/
LSD	26	34	13	27	1	28–30	20–22	17–18	8–9	4	21–25	4
SAU	32–38	30–32	11–12	21–24	6	32–34	16–18	14–15	14–17	8	30–37	9
VAL	37–42	32–34	9–11	16–18	3	29–32	17–19	12–13	11–14	6	36–42	4
POC	28–34	23–29	15–17	22–26	3	35–38	18–20	15–16	16–19	7	32–45	4

[a] Grain-size distribution for the 0/20 mm fraction.
[b] SS: Specific Surface area; *n* is the number of samples; W_l is the liquid limit; W_p is the plastic limit; W_r is the shrinkage limit, I_p is the plasticity index.

the black marl, related to the lack of sensitive clays in the mineralogy. In addition, the consistency parameters of the formations show a direct correlation with the optimum moisture content and an inverse correlation with the maximum dry density (Fig. 5c). This indicates that the clay fraction activity controls the compaction behaviour, as described earlier by several authors on Plaisancian marl from southeast France (Serratrice, 1978) and on Keuper marl from northeast France (Tisot and Houpert, 1980) or by Konomi and Goro (1994).

According to the Universal Soil Classification System (USCS), all the formations can be classified as a porous sandy-silt non-plastic soil. The results of the soil characterisation show that earthflow formations are weathering products in an early stage of development.

4.4. Hydrologic parameters of the reworked and weathered black marl formations

Soil conductivity of the in situ and earthflow formations was tested extensively both in the laboratory (constant and falling head permeameter) and in situ (auger hole tests and tension disk infiltrometer) under pressure or suction. The conductivity values classify the material as semi-permeable (Fig. 6a, Table 3) and are directly related to the formations' grain-size distribution: LSD presents one order of magnitude lower average saturated conductivity values (1.6×10^{-7} ms^{-1}) than USD (1.7×10^{-6} ms^{-1}). Once again, this demonstrated a strong connection between the parent rock and the earthflow formations. The VAL formation contained more silt and presented a higher saturated hydraulic conductivity than the other more clayey formations. These values agree with average results for similar black marl soils in the literature (Caris and Van Asch, 1991; Mulder and Van Asch, 1988a,b; Antoine et al., 1995; Van Asch, 1997; Van Asch and Buma, 1997).

The conductivity values obtained in situ are higher, though more scattered than those in the laboratory tests. They demonstrate that the formations' varying bulk densities do not always correspond to analogous differences in conductivity values. This can mainly be explained by the fact that: (1) the void ratio increase, which should produce an increase in permeability, is probably compensated by the spatial obliteration of the fissures which constitute a preferential water flow path; (2) the soil surface characteristics (size of the embedded elements and crusting) govern the conductivity near saturation (Malet et al., in press) and (3) in situ tests are marked by 3-D effects.

The matric suction–moisture content relationship was obtained using a sand and kaolin box apparatus (Fig. 6b). The behaviour observed is in accordance with the texture of the soils; samples with a higher clay content (USD, LSD, POC, SAU) show a more abrupt change in slope; while the more silty sample of the VAL formation shows a gentler curve. The retention values are high and range from 0.17 to 0.42 cm^3/cm^3.

4.5. Geotechnical tests

4.5.1. Compressibility characteristics of reworked and weathered black marl formations

The compressibility characteristics were determined through laboratory tests carried out on undisturbed soil specimens with a diameter of 70 mm and a

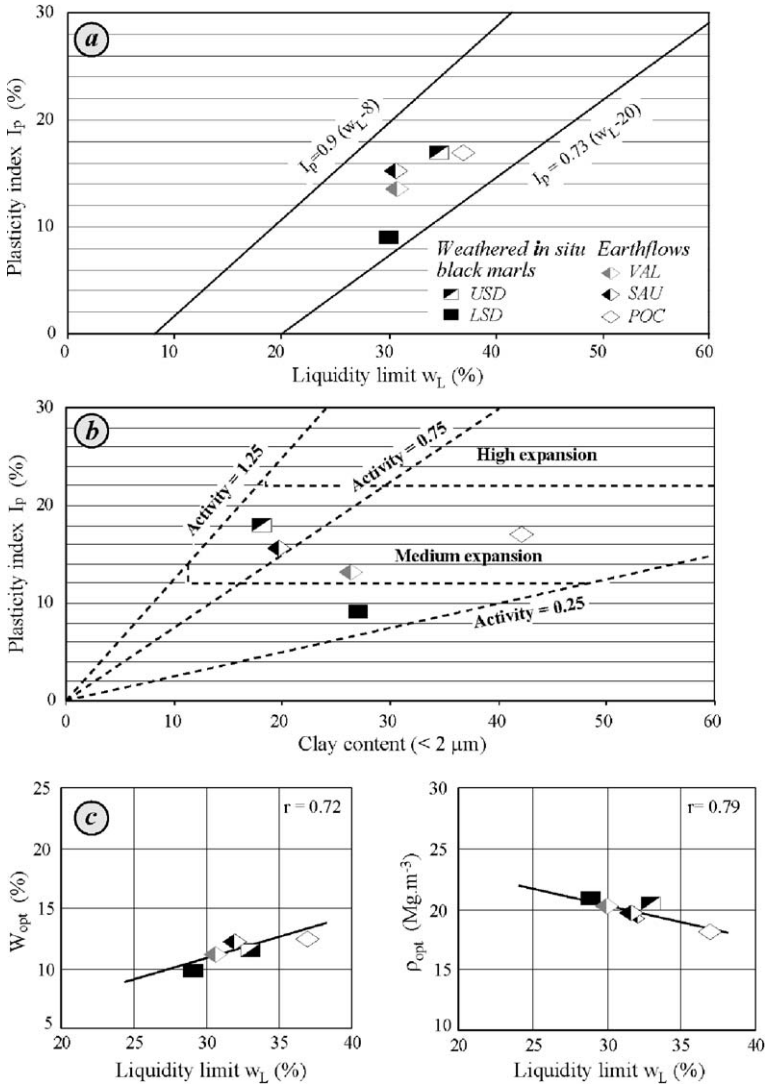

Fig. 5. (a) Casagrande diagram and (b) Skempton activity chart of the different materials. (c) Relation between compaction parameters and Atterberg limits.

height of 24 mm, using a classical Casagrande apparatus with drainage system. Vertical stresses were doubled for each stage beginning with 5 kPa up to 1080 kPa and then decreased in stage by half to 5 kPa. Each stage was maintained for 24 h except the last loading, which was maintained for 1 week or more. Fig. 7 shows typical e vs. log σ' curves. Table 4 shows a summary of the stress–strain parameters (yield stress σ'_p calculated using the Casagrande method and compression index C_c).

The results show a clear change in soil behaviour (rigid to plastic) and a well-defined virgin region can be observed after the yield stress. The USD formation presents a larger initial void ratio ($e_0 \approx 0.8$) but a smaller yield stress ($\sigma'_p \approx 70$ kPa) and compression index ($C_c \approx 0.12$) as compared with the LSD formation ($e_0 \approx 0.5$, $\sigma'_p \approx 110$ kPa and $C_c \approx 0.17$). The POC and SAU formations present higher yield stresses and compression indices than the in situ weathered parent rock. The VAL formation, however, exhibits a

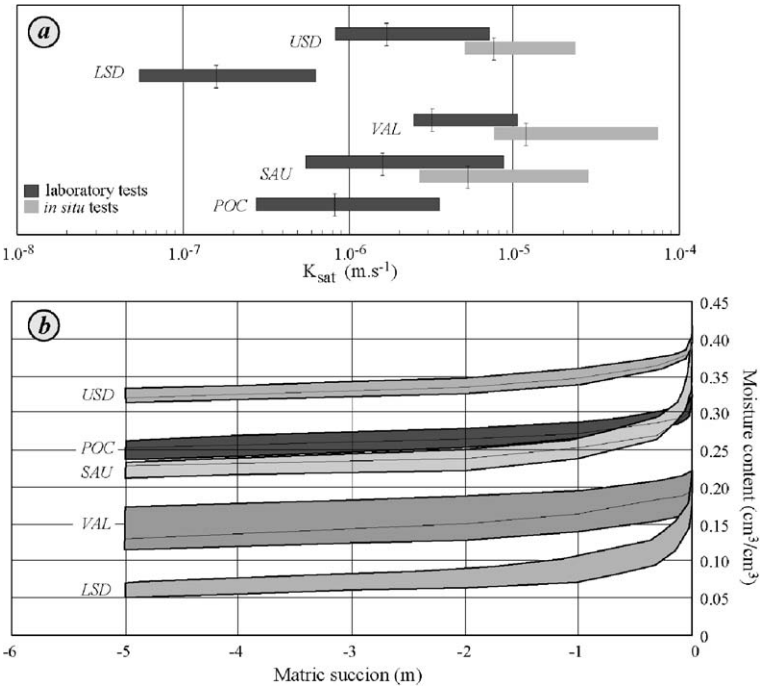

Fig. 6. Hydrological parameters of the formations. (a) Saturated hydraulic conductivity and (b) suction-moisture content relationship.

smaller yield stress and a higher compression index than the in situ weathered parent rock. As the samples were taken at the same depth (0.5 m), this can be explained by the presence of coarser elements (mainly moraine) in the marly matrix. The values of the yield stress for all formations seem strictly correlated to the stress history (from the older deposit to the younger deposit) and to bonding effects caused by weathering. The unloading curves show steeper slopes for the in situ materials, which are more rigid than the earthflow formation (with lower slopes), even under high stresses of 1000 kPa.

Table 3
Hydrological parameters of in situ and reworked (earthflow) materials (field and laboratory tests)

	Conductivity			Retention		
	K_{sat} (m s^{-1})	K_{-100} (m s^{-1})	n	θ_{sat} (cm^3/cm^3)	$\theta_{pF\ 2.7}$ (cm^3/cm^3)	n
USD	1.7×10^{-6}	7.6×10^{-7}	39	0.37–0.42	0.32–0.34	27
LSD	1.6×10^{-7}	6.7×10^{-8}	27	0.16–0.22	0.05–0.08	18
SAU	1.4×10^{-6}	3.3×10^{-6}	165	0.33–0.40	0.21–0.24	129
VAL	4.1×10^{-6}	1.8×10^{-6}	58	0.17–0.23	0.11–0.18	36
POC	8.2×10^{-7}	4.3×10^{-8}	86	0.28–0.34	0.23–0.27	42

K_{sat} is the saturated hydraulic conductivity (geometric average); K_{-100} is the unsaturated hydraulic conductivity for a pressure head of -100 mm (geometric average); n is the number of measurements; θ_{sat} is the retention capacity at saturation; $\theta_{pF\ 2.7}$ is the retention capacity at pF 2.7.

The primary settlement occurs almost immediately in all tests and lasts only a very short time, especially for the USD formation and the earthflows developed in it (SAU, VAL). This feature can be explained by the relatively higher porosity of this formation, which allows water to drain quickly. The secondary compression or creep is characterised by a continuing small increase in vertical strain and may be generated by several processes (ongoing locking of the soil structure after the primary compression, fracturing of the individual calcite particles and failure of the argillaceous bonds; Lambe and Whitman, 1979). The results of long duration oedometer tests on the SAU material indicate that the creep effect during the secondary compression phase continues over weeks and even months. Similar behaviour was described in geotechnical studies of other marly soils from Southeast France (Phan, 1993; Serratrice, 1995; Magnan and Serratrice, 1995).

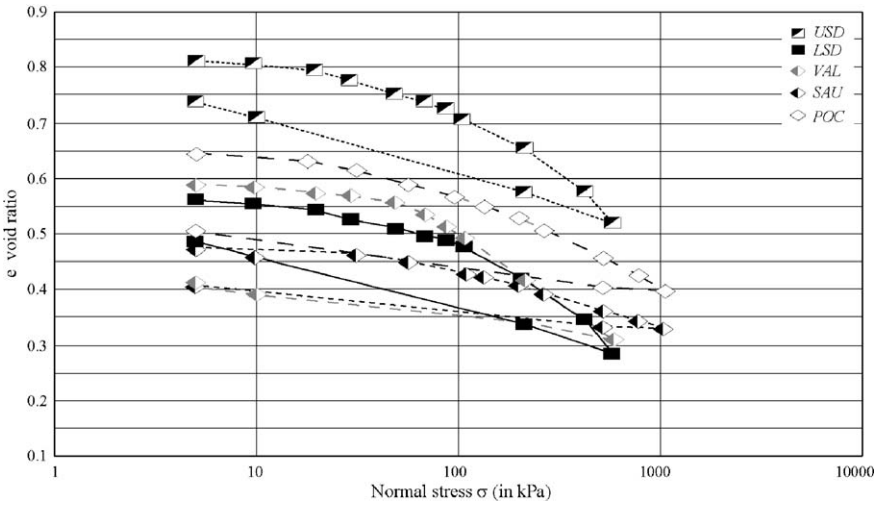

Fig. 7. Vertical stresses-void ratio curves for different loadings.

4.5.2. Strength properties of reworked and weathered black marl formations

Cylindrical specimens with a diameter of 68 mm and a height of 30 mm were carefully trimmed for direct shear box testing. Moisture contents were generally low, varying from 8% to 15%. The applied normal stress varied from 31 to 300 kPa at low shearing velocity. Shearing tests were carried out after a 24-h consolidation phase.

The stress-strain curves (Fig. 8a–f) show an asymptotic shape, the absence of a peak and a high level of residual strength. This type of plastic failure for normally consolidated materials is not specific to the marl in the Barcelonnette Basin and has been observed by several authors (Phan, 1993; Colas and Locat, 1993; Van Beek and Van Asch, 1996). It is caused by particle reorganization and progressive compaction. Pre-failure displacements were relatively low (from 2% to 3% of the diameter of the sample). LSD specimens only seemed to develop a small peak for normal stresses lower than 200 kPa and for small deformations (Fig. 8f); the shear strength increased, then decreased to a constant volume strength. In contrast, above normal stresses of 200 kPa, the specimen failed in an essentially plastic fashion. It seems that the marl in the lower part of the stratigraphy (LSD) has undergone long-term consolidation and compaction, and subsequently suffered to some extent from unloading arising from denudation. It therefore showed a relatively overconsolidated state. The presence of a peak in the stress–strain curves can also be related to specific problems due to the presence of coarse particles and clasts in the specimens. These considerations will be discussed in Section 5 of this paper.

Table 4
Compressibility and strength properties of reworked and weathered black marl formations

	Oedometer tests			Direct shear tests			Ring shear tests		
	C_c	σ'_p (kPa)	n	φ' (°)	c' (kPa)	n	φ'_r (°)	c'_r (kPa)	n
USD	0.11–0.14	68–76	5	30–33	15–22	7	/	/	/
LSD	0.16–0.19	106–119	4	34–39	8–17	9	/	/	/
SAU	0.10–0.13	85–92	12	29–32	16–37	10	22–25	3–7	11
VAL	0.29–0.32	48–63	8	21–24	31–40	9	19–21	10–14	11
POC	0.15–0.17	133–146	7	28–37	8–22	7	24–27	4–8	11

C_c is the compression index; σ'_p is the preconsolidation stress; n is the number of measurements; φ' is the effective angle of friction; c' is the effective cohesion; φ'_r is the residual angle of friction; c'_r is the residual cohesion.

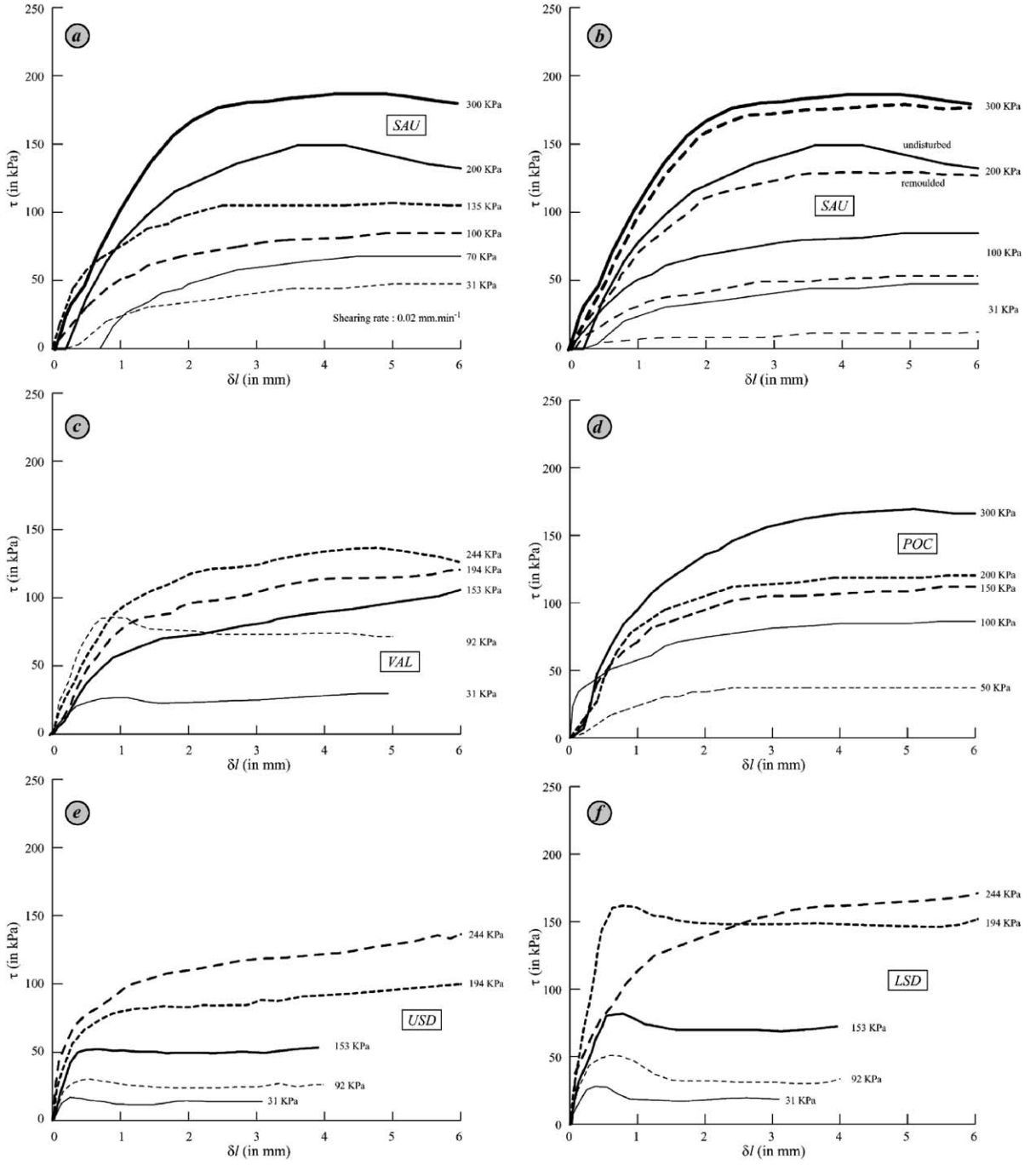

Fig. 8. (a) Stress–strain diagram (drained direct shear tests) of the SAU earthflow reworked marl; (b) Effects of bonding on the SAU earthflow reworked marl. Stress–strain diagram for undisturbed and remoulded specimens; (c) stress–strain diagram of the VAL earthflow reworked marl; (d) stress–strain diagram of the POC earthflow reworked marl; (e) stress–strain diagram of the USD weathered marl; (f) stress–strain diagram of the LSD weathered marl.

Since displacements directly following failure of the specimens tested in the direct shear box were high, it was not possible to obtain any reliable data on the post-peak strength. However, we know that slope failure occurs within old failed bodies and along discrete zones within the marl slopes where progressive weathering has affected the marly fabric (Antoine et al., 1995); a combination of peak strength and residual strength values is necessary, therefore, for marly slopes characterised by fissures, gypsum efflorescences, ridges in the terrain or other indicators of weathering and/or movement, in order to obtain realistic results from stability analyses (Leroueil, 2001).

The effect of bonding was analysed by comparing data from undisturbed and remoulded SAU specimens (Fig. 8b), sheared by applying low and high normal stresses (31 and 300 kPa). No peak was observed and the remoulded specimens showed a plastic type of failure. Moreover, there was no significant difference between the curves obtained from the undisturbed and the remoulded specimens under high normal stresses; the similar strength values for the two specimens tested indicate that the bonding had already been disintegrated during the consolidation phase when high normal stress was applied. However, the undisturbed and remoulded specimens gave very different results when low normal stresses were applied (<200 kPa). The strength of the undisturbed specimen clearly exceeds that of the remoulded specimen; the bonded structure of the soil apparently remaining intact in the undisturbed specimen. Similar behaviour was revealed by direct shear testing of Pyrenean marl by Camapum de Carvalho (1985).

Manually remoulded specimens (fraction 0/20 mm) were tested using a modified Bromhead ring shear apparatus, in which a series of small vanes were attached to the top and bottom platen (Bromhead, 1979; Boyce et al., 1988). This test is extremely useful for obtaining information on the residual strength of the marl and the effects of moisture content on the apparent effective cohesion and effective angle of friction. For this purpose, water was subsequently added to air-dried specimens until the required moisture content was achieved. Before shearing, the remoulded specimen was consolidated to the effective normal stress of 200 kPa, a value chosen to represent field conditions. Specimens of the three earthflows were sheared at 0.6 mm min^{-1} under drained conditions, following the procedure of Anayi et al. (1989).

The initial moisture content ranged from 3% to more than 30%. The points plotted in Fig. 9 represent effective stress-strength parameters that have been corrected according to the amount of water lost during shearing. We believe that the residual strength parameters are dependent only on the final moisture content. The distribution of the data leads us to conclude that there is a linear relationship between the residual cohesion and the moisture content, whereas the relationship of the residual angle of friction with increasing moisture content is

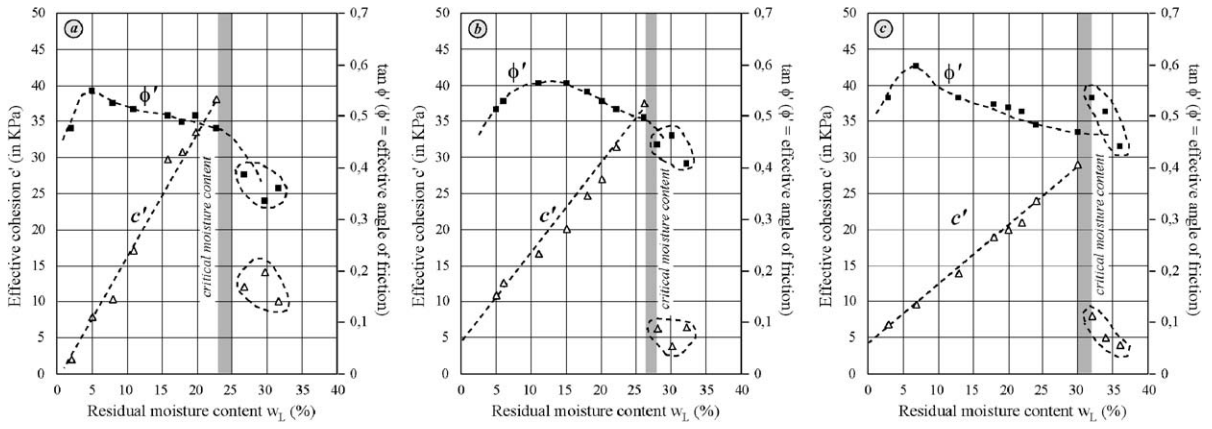

Fig. 9. Changes in apparent cohesion and effective angle of friction against the variation of moisture content (modified Bromhead ring shear apparatus) for (a) VAL, (b) SAU and (c) POC earthflows.

more complex as noted by Dijkstra et al. (1994) for loess formations. An increase in the residual angle of friction can be observed in all three cases up to a moisture content of 5–10%. The residual angle of friction declines thereafter and the curve gradually flattens out at moisture contents of just under 30%. The residual cohesion falls abruptly when the same moisture content is present.

The three earthflow formations respond in a similar way in the ring shear tests. The critical moisture content is highest for the POC specimen (near 30%), followed by the SAU specimen (27–28%) and the VAL specimen (25%). These characteristic moisture contents are related to the liquid limit of these formations. Manual remoulding has eliminated the characteristic structure of the undisturbed sediments, such as the degree of compaction and cementation. The differences between the samples must therefore relate to changes in the shape, size and surface roughness of the particles, and to a lesser extent to mineralogy. Under air dry conditions, the effective angle of friction is determined simply by the degree of interlocking of the particles. The clay particles form absorption membranes when water is added and further increases in the moisture content increase the thickness of the membranes. This causes the effective angle of friction to decrease. The capillary menisci continue to grow as the soil moisture content increases until a steady state is reached; this seems to be related to the liquid limit of the formation and the applied normal effective stress (Dijkstra et al., 1994).

As expected, the residual values of all samples are broadly similar and about one third of the values obtained in the direct shear tests (Table 4). This is discussed below.

5. Discussion: geomechanical behaviour of the marl and implications for landslide susceptibility

5.1. A specific protocol to characterise the geomechanical behaviour of the black marl

These marly materials evolving under the action of hydrometeorological processes are at varying stages of development, depending on the age and the lithological characteristics of the earthflows. The heterogeneity of the formations and the strong erodability of the marly fragments during testing also required specific protocols to represent their geomechanical behaviour, the more so as our main objective was to describe the behaviour of the weathered material in situ and the reworked earthflow formations, where small differences exist.

These methodological problems arise in particular when determining representative grain size distributions (choice of sampling sites, value of D_{max}, volume or weight of the samples; Kellerhalls and Bray, 1971; Hey and Thorne, 1983; Meunier and Carion, 1987) or representative strength characteristics. The various grain size distributions published for the black marl of the Barcelonnette Basin) stress the importance of the silty fraction, (Caris and Van Asch, 1991; Phan, 1993; Phan and Antoine, 1994; Antoine et al., 1995; Locat, 1997; Le Mignon, 1999; Remaître et al., 2002) but the strong dispersion of the clayey fraction obtained by these authors (from 15% to 45%), makes comparisons and interpretations delicate. Does this dispersion translate the high heterogeneity of the formations or is it related to a bias introduced by the testing protocol? The objective of the analyses (i.e. to characterise the total granulometric spectrum, or only one particular fraction) is also important.

The fraction 0/20 mm accounts for 45–60% of the $0/D_{max}$ (Malet et al, submitted for publication, a,b), depending on the formations. Thus, it seems essential, on the one hand, to carry out these analyses on an optimal volume of 0.04–0.05 m^3 (i.e. a mass of 80–100 kg) to define the proportion of silt and clay accurately, and on the other hand to avoid forming artificially fine particles during testing because of the brittleness of the marly clasts. For instance, Antoine et al. (1995) and Herrmann (1997) showed that wet sieve analysis led to a total dissociation of the material, accompanied by a certain change in the shape of the grain size distribution, as compared with dry sieve analysis. The curves tend to shift finer, which indicates a reduction in the mean particle size and thus an overestimation of the clay-silt percentage (>80%), at odds with the field observations. Phan (1993) showed that the marl could release 80% fine particles by wet sieving, whereas they release only 2% by dry sieving.

Indeed, the use of standardized protocols based on the grain size distribution of quartz sands which do not weaken throughout sieving (Rivière, 1977), results

in the fragmentation of the clay aggregates in contact with water by repeated impacts on the different sieves. It is for these reasons that we propose a specific protocol for this type of material. The sieving must be soft and delicate to limit the number of collisions between the particles.

The same care must be taken in determining the strength characteristics of the black marl. Strength envelopes were plotted using the results obtained from all direct shear tests after a meticulous interpretation of the stress–strain curves (Fig. 10). The envelopes are best-fit straight lines through the final state stresses (i.e. as no peak was observed, the stresses corresponding to the final state were determined). The angles of friction and cohesion values were then determined by applying the Mohr–Coulomb failure law (Lambe and Whitman, 1979).

The ranges of results were relatively narrow for the SAU formation ($\varphi' = 29–32°$) and the VAL formation ($\varphi' = 21–24°$), and wide for the POC formation ($\varphi' = 28–37°$), due to its wider dispersion. The effective cohesion was between 6 and 40 kPa. The earthflow formations presented lower friction angles and higher effective cohesions than the associated weathered in situ parent rock; this was related to the weathering, which contributes to the creation of argillaceous bonds in the matrix and reduces the friction between the particles.

The three earthflows can be classified according to their age by the friction angles: the VAL earthflow exhibits the lowest friction angles and the POC earthflow the highest. The scatterplot for each formation is well bounded by the limiting failure envelopes (Fig. 10). The strengths are in accordance with those of Antoine et al. (1995) for black marl colluvium (mean $c' = 13$ kPa, $\sigma^2 = 49$ kPa; mean $\varphi' = 35°$, $\sigma^2 = 4°$ from 131 drained direct shear tests).

All these tests confirm the slope stability back-analyses by Antoine et al. (1988) on six landslides involving black marl, which gave friction angles of $29 \pm 2°$ and cohesions of 72 ± 13 kPa. These values are also consistent with the drained triaxial tests of Antoine et al. (1995), despite the high standard deviations (mean $c' = 12$ kPa, $\sigma^2 = 243$ kPa; mean $\varphi' = 25°$, $\sigma^2 = 0.5°$ from 19 tests).

This being so, we were obliged to carry out a significant number of tests to avoid experimental bias due to the presence of a marly or calcite fragment in the shear box, in order to obtain realistic strength values. Finally, it is advisable not to attach too much importance to the variations in the cohesion values, firstly, because the cohesion due to the carbonated

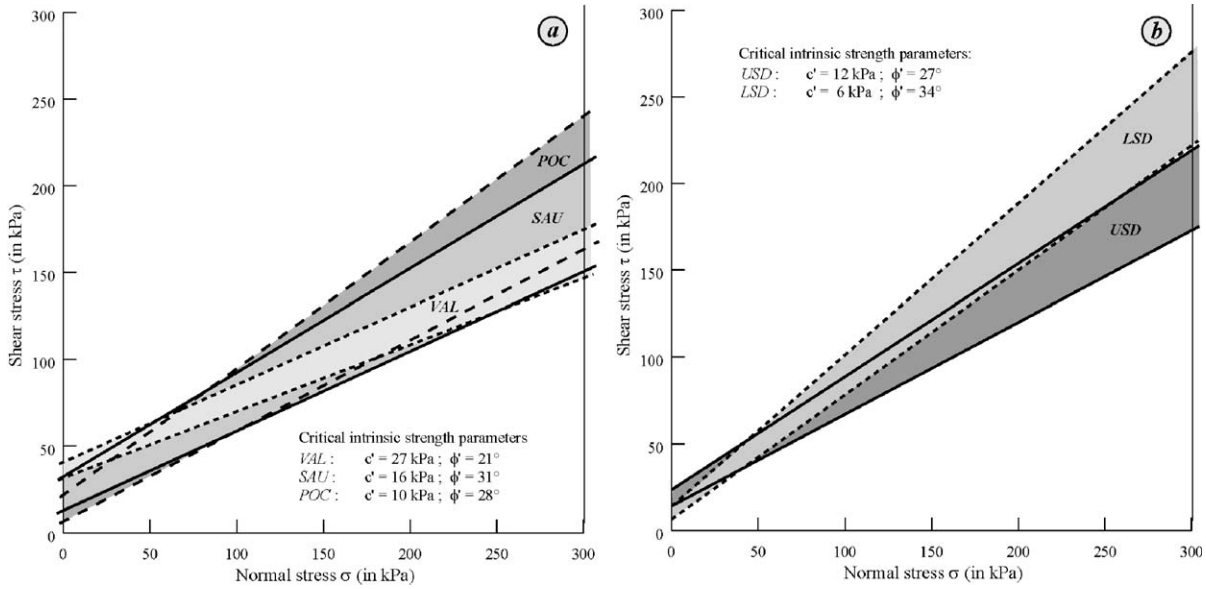

Fig. 10. Mohr–Coulomb failures planes of (a) the reworked earthflow formations and (b) the in situ weathered formations.

bridges decreases on soaking, which destroys the majority of the bonds (Phan, 1993), and secondly, because shear resistance due to cohesion is only mobilized for small displacements; the friction between the particles governs the strength for large displacements.

5.2. Short- and long-term evolution of landslides: relationships between weathering, strength, slope instability and initiation of rapid mass movements

Once the validity of the grain size distributions and strength values has been established, relationships between weathering, strength, slope instability and initiation of mass movements can be evaluated. Generally, assuming no pore pressures, failure only occurs on a natural slope if the slope angle exceeds the formation's friction angle for zero cohesion and in the absence of external forces. The residual friction angles of the reworked black marl range between 20° and 25°, and they have a relatively low cohesion (5–15 kPa). The earthflows were therefore examined for stability, assuming 8-m deep sliding surfaces. The stability of the slopes subjected to this translational sliding can be evaluated using Infinite Slope Analysis. Skempton and DeLory's (1957) equation for Infinite Slope Analysis was modified for the present case as follows:

$$F_s = \frac{c' + [\gamma Z - m\gamma_w Z]*\cos^2\beta*\tan\phi'}{\gamma Z*\sin\beta*\cos\beta} \quad (1)$$

where γ and Z denote, respectively, the saturated unit weight of the formation and the thickness of the failing soil, F_s is the factor of safety, γ_w is the unit weight of water, β is the slope angle, c' and ϕ' are the cohesion and the angle of internal friction, and m is the fraction of Z such that mZ is the vertical height of the groundwater table above the sliding surface. Using residual strength parameters in Eq. (1), relationships between F_s and β were obtained (Fig. 11) for various m values ($m=0$, no water table; $m=1.0$, water table at the slope surface). The groundwater table for the actual slopes fluctuates between half the depth of the sliding mass ($m=0.5$) and the slope surface ($m=1.0$).

Under critical conditions, $F_s=1.0$, and assuming $m=0.5$, the maximum stable slope angles for residual strength (Table 4) reach 21° for the VAL and SAU earthflows, and 23° for the POC earthflow. The slope angles decreased to 16° and 18° for fully saturated conditions. As the mean topographic slopes of the three earthflows lie directly in this range, the flow can accelerate under observed rainfall and snowmelt conditions and each can be characterised as very active. The result of this analysis is compatible with the results of in situ measurements which show that the earthflows are inactive when the groundwater is very low (less than half the depth of the slide), and active when the groundwater table rises above half the depth of the slide (Fig. 11; Malet et al., 2002a). The POC earthflow is the more stable, as the topographic slope and the mean annual position of the groundwater table are lower; the relative stability of this earthflow is also explained by an evolution of the strength of the material due to weathering.

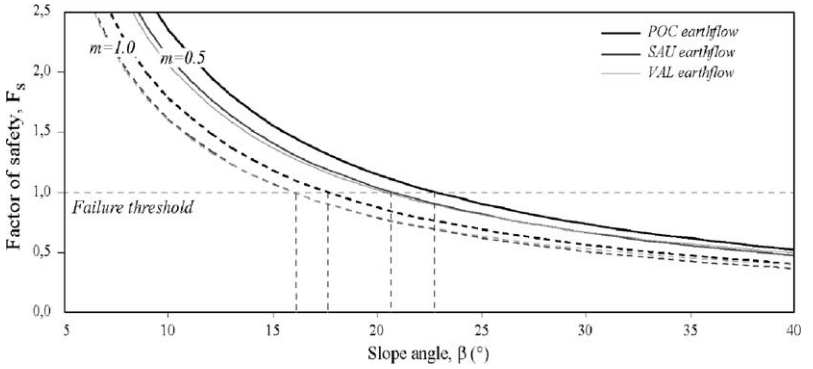

Fig. 11. Relationship between slope angle β, and factor of safety, F_s, for two m-values for residual shear strengths of the VAL, SAU and POC earthflows.

The laboratory tests demonstrated a strong correlation between the in situ weathered parent rock (USD or LSD) and the earthflow formations. The grain size distributions of the earthflow deposits (Fig. 4c) show an increase in either the silt or clay fraction from the most recent earthflow (VAL) to the oldest (POC). This characteristic has a considerable effect on the hydrological behaviour of the superficial layers of the earthflows (Tables 2 and 3) (porosity, conductivity and retention capacity).

The POC formation must therefore be more cohesive than the SAU and VAL formations, not taking into account the specific lithological nature of each earthflow. With time, the residual angle of friction increases gradually and stabilises to a constant value, while the residual cohesion decreases and stabilises at a certain level (Fig. 12a). Surprisingly, in the long-term, the material seems to become more frictional and less cohesive. The reduced cohesion can be attributed to the deterioration and the dissolution of the carbonated and argillaceous bonds over a period of time. The increased angle of friction is more surprising, as the formation of fine particles by weathering should reduce it. Presumably, it is complex chemical alteration which determines the transformation or the neoformation of clay minerals, which tend to increase the overall strength and specific research should be carried out on that particular point. This long-term rearrangement results in a direct increase in strength and in the collapse in pores. It is not surprising, therefore, that the older the earthflow, the lower the conductivity.

An idealized diagram representing the long-term evolution of marly hillslopes characterised by the presence of earthflows can be constructed (Fig. 12b) on the basis of the Infinite Slope Model (Matsukura, 1996). It illustrates the concept of stability/instability in these slopes by combining: (1) the evolution of strength with time, initially marked by strength reduction with

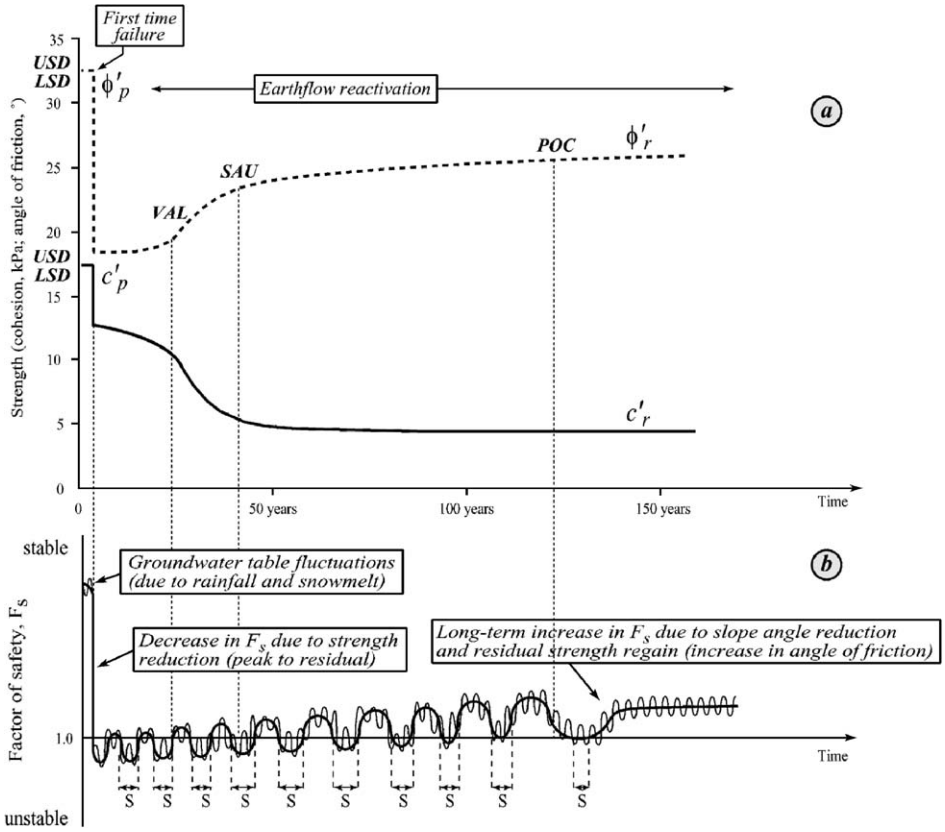

Fig. 12. The changes in (a) residual soil strength and (b) safety factor F_s for a long period.

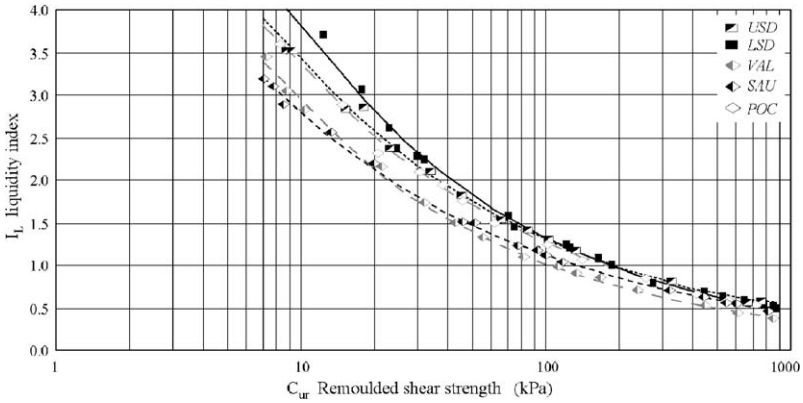

Fig. 13. Remoulded undrained shear strength vs. liquidity index for the different materials.

first-time failures (from peak strength to residual strength values), and then by progressively regaining strength due to the increase in the residual angle of friction; (2) the slope angle changes for a long period; and (3) pore pressures fluctuations in relation to rainfall. Under present climactic conditions, black marl earthflows may be active for decades or more, with a behaviour near $F_s = 1$, and then progressively stabilize after a 150-year period. These considerations relate to the higher velocities monitored on the VAL earthflow rather than those on the POC earthflow. It is difficult, however, to predict exactly when the slope will become unstable, causing renewed movement, because of the lack of data on the rate of weathering.

Nevertheless, some parts of the three earthflows can trigger debris-flows (Malet et al., 2002b, submitted for publication, a,b). The susceptibility to debris-flow initiation can be evaluated from a plot of undrained shear strength versus liquidity index, as undrained shear strength gives a good estimate of the material's yield stress (Locat and Demers, 1988; Locat, 1997). Fig. 13 shows that more water is necessary to initiate debris-flow in the POC than in the SAU and VAL earthflows. This must nevertheless be confirmed by rheological tests on the same formations (Malet et al., 2002b).

6. Conclusions

The black marl in Southeastern France consists of easily weathered and erodable material. These characteristics make it particularly prone to erosion and mass-movements and also calls for particular care in determining representative hydrological and geomechanical parameters. The following conclusions may be drawn from the results and discussion presented here.

(1) Particular care and specific procedures should be used to define the behaviour of the evolving black marl and the heterogeneity of the formation, mixing coarse materials and argillaceous aggregates.
(2) The behaviour of the black marl under load results in an immediate packing followed by a secondary packing phase. The saturation of the material results in swelling under low stresses (< 220 kPa), or the resumption of packing under high stresses, leading to structural collapse of the material.
(3) The in situ Upper Stratigraphic Deposit (USD) and the reworked formations fail plastically under both low and high normal stresses, while the Lower Stratigraphic Deposit (LSD) exhibits a more brittle failure under normal stresses of 200 kPa because it is more cemented.
(4) The behaviour of the remoulded black marl differs markedly from the behaviour of the undisturbed black marl, until a threshold is reached. Above a normal stress of 200 kPa, the strength generated by bonding is missing and the stress-strain curves do not differ between undisturbed and remoulded specimens.

(5) As the water content of the black marl rises, the effective apparent cohesion rises proportionately up to a limit of 30–40 kPa at a water content of 30–35%, after which the value falls rapidly to a much lower level.
(6) The effective angle of friction rises to a water content of approximately 5–10% and thereafter falls to a lower value at approximately 25–30%.
(7) Surprisingly, weathering of the black marl results in a progressive regain of strength in the long-term, due to the increase of the residual angle of friction, possibly related to chemical alteration of the clay minerals.
(8) An idealized diagram illustrating the relationship between weathering, strength and slope instability of black marl hillslopes has been constructed and the overall stability of the earthflows can be well explained by the infinite slope stability analysis.
(9) Strong relationships exist between the behaviour of the weathered source material and the earthflow developed in it.
(10) Finally, taking into account the heterogeneity of the formations, the strength parameters appropriate for slope stability analysis and risk assessment are the lowest effective strength values ($c'=0$ kPa, $\varphi'=25-28°$).

Acknowledgements

This program was supported by the Centre National de la Recherche Scientifique (CNRS) within the framework of INSU-PNRN (Contracts 97/99-34MT and ECLAT Ecoulement, initiation et Contribution des LAves Torrentielles dans les bassins marneux-) and the French Ministry of Research within the ACI-CatNat Contract MOTE (MOdélisation, Transformation, Ecoulement des coulées boueuses dans les marnes). Contribution INSU No. 332. Contribution EOST No. 2003.027-UMR7516. The authors wish to thank D. Herrmann, J. Genet, S. Pierre, A. Puissant, A. Ritzenthaler, M. Schmutz, O. Trisse, E. Truchet, S. Velcin and D. Weber for their precious help in the field, Professor J.-C. Flageollet who encouraged this research, M. Trautmann for her assistance in the laboratory tests, and Professor J.D. Williams (University of Queensland, Australia) and an anonymous referee for their valuable comments. Very special thanks are due to Mrs. Margaret Nelson for the reviewing of the English version of the paper.

References

Alexandre, A., 1995. Suivi expérimental du ravinement des marnes dans les Baronnies. Travaux du Laboratoire de Géographie Physique 23, 154 (Paris).

Anayi, J.T., Boyce, J.R., Rogers, C.D.F., 1989. Modified Bromhead ring shear apparatus. ASTM, Geotechnical Testing Journal 12 (2), 121–130.

Antoine, P., Fabre, D., Giraud, A., Al Hayari, M., 1988. Propriétés géotechniques de quelques ensembles géologiques propices aux glissements de terrains. Proceedings of the Vth International Symposium on Landslides, Lausanne, vol. 2. Balkema, Rotterdam, pp. 1301–1306.

Antoine, P., Giraud, A., Meunier, M., Van Asch, T., 1995. Geological and geotechnical properties of the "Terres Noires" in the southeastern France: weathering, erosion, solid transport and instability. Engineering Geology 40, 223–234.

Artru, P., 1972. Les Terres Noires du bassin rhodanien (Bajocien supérieur à Oxfordien moyen): stratigraphie, sédimentologie, géochimie. PhD Thesis, Lyon III University. 182 pp.

Awongo, M.-L., 1984. Stratigraphie, sédimentologie et géochimie des Terres Noires du Jurassique moyen et supérieur de la Provence (sud-est de la France). PhD Thesis, Marseille III University. 144 pp.

Boyce, J.R., Anayi, J.T., Rogers, C.D.F., 1988. Residual strength of soils at low normal stresses. Proceedings of the Vth International Symposium on Landslides, Lausanne, vol. 1. Balkema, Rotterdam, pp. 85–88.

Bromhead, E.N., 1979. A simple ring shear apparatus. Ground Engineering 15 (5), 40–44.

B.R.G.M. (Bureau des Recherches Géologiques et Minières), 1974. Barcelonnette. Notice Géologique de la carte XXXV-39.

Bufalo, M., 1989. L'érosion des Terres Noires dans la région du Buëch (Hautes-Alpes, France). PhD Thesis, Aix-Marseille University. 230 pp.

Camapum de Carvalho, J., 1985. Étude du comportement d'une marne noire compactée. PhD Thesis, Toulouse I University. 181 pp.

Caris, J.P.T., Van Asch, T., 1991. Geophysical, geotechnical and hydrological investigations of a small landslide in the French Alps. Engineering Geology 31, 249–276.

Casagrande, A., 1932. Research on the Atterberg limits of soils. Public Roads 13 (8), 131–136.

Chodzco, J., Lecompte, M., Lhenaff, R., Marre, A., 1991. Vitesse de l'érosion dans les "Roubines" des Baronnies (Drôme). Physio-Géo, 22-23, 21–28.

Colas, G., Locat, J., 1993. Glissement et coulée de La Valette dans les Alpes de Haute-Provence: présentation générale et modélisation de la coulée. Bulletin de Liaison du Laboratoire des Ponts et Chaussées 187, 19–28.

Coulmeau, P., 1987. Quelques éléments sur la géomorphologie et

les processus érosifs observés dans le bassin du Laval. Les bassins versants expérimentaux de Draix, Compte-Rendu de Recherche No. 1 en Erosion et Hydraulique Torrentielle. Cemagref, Grenoble. 128 pp.

Cullity, B.D., 1989. Elements of X-ray Diffraction. Addison-Wesley Publishing, Reading, MA. 514 pp.

Descroix, L., Olivry, J.C., 2002. Spatial and temporal factors of erosion by water of black marl in the badlands of the French Southern Alps. Hydrological Sciences Journal 47 (2), 227–242.

Dijkstra, T.A., Rogers, C.D.F., Smalley, I.J., Derbyshire, E., Jin, L.Y., Min, M.X., 1994. The loess of north-central China: geotechnical properties and their relation to slope stability. Engineering Geology 36, 153–171.

Flageollet, J.-C., Maquaire, O., Weber, D., 1996. The temporal stability and activity of landslides in Europe with respect to climatic change (TESLEC), Final National Report. In: Dikau, R., et al. (Eds.), C.E.C. Environment Program, Contract EV5V-CT94-0454. EU, Brussels, pp. 126–186.

Flageollet, J.-C., Maquaire, O., Weber, D., Martin, B., 1999. Landslides and climatic conditions in Barcelonnette and Vars Basin (Southern Alps, France). Geomorphology 30, 65–78.

Flageollet, J.-C., Malet, J.-P., Maquaire, O., 2000. The 3-D Structure of the Super-Sauze earthflow: a first stage towards modelling its behaviour. Physics and Chemistry of the Earth (B) 25 (9), 785–791.

Garnier, P., Lecompte, M., 1996. Essai sur les mécanismes de fragmentation des marnes des Baronnies (France). Géomorphologie: Relief, Processus, Environnement 1, 23–50.

Gerrits, J., Imeson, A.C., Verstraten, J.M., Bryan, R.B., 1987. Rill development and badland regolith properties. Catena Supplement 8, 141–160.

Guillon, J., 2001. Interprétation morphologique de l'évolution du glissement-coulée de Poche et caractérisation physico-mécanique des matériaux marneux (Alpes-de-Haute-Provence, France). Master Thesis, Strasbourg I University. 118 pp.

Hansbo, S., 1957. A new approach to the determination of the shear strength of clay by the fall-cone test. Internal Report, Swedish Geotechnical Institute. 47 pp.

Harvey, A.M., Calvo, A., 1991. Process interactions and rill development on badland and gully slopes. Zeitschrift für Geomorphology, SupplementBand 83, 175–194.

Herrmann, D., 1997. Recherches des caractéristiques physiques et géotechniques des Terres Noires du glissement de terrain de Super-Sauze (Alpes-de-Haute-Provence). Master Thesis, Strasbourg I University. 127 pp.

Hey, J.K., Thorne, G.H., 1983. Accuracy of surface samples from gravel bed material. ASCE Journal of Hydraulic Engineering 109 (2), 41–77.

Imeson, A.C., Verstraten, J.M., 1988. Rills on badland slopes: a physico-chemical controlled phenomenon. Catena Supplement 12, 139–150.

Kellerhalls, H., Bray, R.F., 1971. Sampling procedures for coarse fluvial sediments. ASCE Journal of Hydraulic Division 71 (2), 51–83.

Konomi, N., Goro, N., 1994. Type génétique des argiles et des marnes et leur compactage dynamique. Proceedings of the VIIth International Congress of the International Association of Engineering Geology, Lisboa, vol. 2. Balkema, Rotterdam, pp. 521–526.

Lambe, T.W., Whitman, R.V., 1979. Soil Mechanics. Wiley, New York. 553 pp.

Lecarpentier, C., 1963. La crue de juin 1957 et ses conséquences morphodynamiques. PhD Thesis, Strasbourg I University. 319 pp.

Légier, A., 1977. Mouvement de terrain et évolution récente du relief dans la région de Barcelonnette (Alpes-de-Haute-Provence). PhD thesis, Grenoble I University. 163 pp.

Le Mignon, G., 1999. Glissements et coulées boueuses: analyse et modélisation. Application au cas de La Valette. DEA Thesis, Ecole Nationale Supérieure des Mines. Paris. 45 pp.

Leroueil, S., 2001. Natural slopes and cuts: movement and failure mechanisms. Géotechnique 51 (3), 197–243.

Locat, J., 1997. Normalized rheological behaviour of fine muds and their flow properties in a pseudoplastic regime. Proceedings of the Ist International conference on Debris-Flow Hazards Mitigation, San Francisco. ASCE, New York, pp. 260–269.

Locat, J., Demers, D., 1988. Viscosity, yield stress, remoulded strength and liquidity index relationships for sensitive clays. Canadian Geotechnical Journal 25, 799–806.

Magnan, J.-P., Serratrice, J.-F., 1995. Détermination de la courbe d'état limite d'une marne. Proceedings of the XIth European Congress of Soil Mechanics and Foundation Engineering, Copenhague, vol. 2. Danish Geotechnical Society, Copenhague, pp. 167–172.

Malet, J.-P., Maquaire, O., Klotz, S., 2000. The Super-Sauze flowslide (Alpes-de-Haute-Provence, France): triggering mechanisms and behaviour. Proceedings of the VIIIth International Symposium on Landslides, Cardiff, vol. 2. T. Telford, London, pp. 999–1006.

Malet, J.-P., Maquaire, O., Calais, E., 2002a. The use of Global Positioning System for the continuous monitoring of landslides. Application to the Super-Sauze earthflow (Alpes-de-Haute-Provence, France). Geomorphology 43, 33–54.

Malet, J.-P., Remaître, A., Ancey, C., Locat, J., Meunier, M., Maquaire, O., 2002b. Caractérisation rhéologique des coulées de débris et laves torrentielles du bassin marneux de Barcelonnette (Alpes-de-Haute-Provence, France). Rhéologie 1, 17–25.

Malet, J.-P., Auzet, A.-V., Maquaire, O., Ambroise, B., Descroix, L., Estèves, M., Vandervaere, J.-P., Truchet, E., in press. Investigating the influence of soil surface features on infiltration on marly hillslopes. Application to Callovo–Oxfordian black marl slopes in the Barcelonnette basin (Alpes-de-Haute-Provence, France). Earth Surface Processes and Landforms. 23 pp. (accepted).

Malet, J.-P., Locat, J., Remaître, A., Maquaire, O., submitted, a. Triggering conditions and mobility of debris-flows associated to complex earthflows. The case of the Super-Sauze earthflow (South Alps, France). Geomorphology (20 pp., in review).

Malet, J.-P., Remaître, A., Maquaire, O., Ancey, C., Locat, J., submitted, b. Flow susceptibility of heterogeneous marly formations. Implications for torrent hazard control in the Barcelonnette basin (Alpes-de-Haute-Provence, France). In: Rickenmann, D., Chen, C.-L. (Eds), Proceedings of the IIIrd International Conference on Debris-Flow Hazard Mitigation: Mechanics, Prediction and As-

sessment, Davos (Switzerland), 10–15 September 2003. 12 pp. (in review).

Maquaire, O., Flageollet, J.-C., Malet, J.-P., Schmutz, M., Weber, D., Klotz, S., Albouy, Y., Descloîtres, M., Dietrich, M., Guérin, R., Schott, J.-J., 2001. Une approche multidisciplinaire pour la connaissance d'un glissement-coulée dans les marnes noires (Super-Sauze, Alpes-de-Haute-Provence, France). Revue Franç aise de Géotechnique 95/96, 15–31.

Maquaire, O., Ritzenthaler, A., Fabre, D., Thiery, Y., Truchet, E., Malet, J.-P., Monnet, J., 2002. Caractérisation des profils de formations superficielles par pénétrométrie dynamique à énergie variable: application aux marnes noires de Draix (Alpes-de-Haute-Provence, France). Comptes-Rendus Geosciences 334, 835–841.

Martínez-Mena, M., Castillo, V., Albaladejo, J., 2002. Relations between interril erosion processes and sediment particle size distribution in a semiarid Mediterranean area of Southeast Spain. Geomorphology 45, 261–275.

Matsukura, Y., 1996. The role of the degree of weathering and groundwater fluctuation in landslide movement in a colluvium of weathered hornblende-gabbro. Catena 27, 63–78.

Meunier, M., Carion, C., 1987. Etude méthodologique de la détermination des courbes granulométriques des lits des cours d'eau. Intenal Report, Cemagref, Grenoble. 30 pp.

Mulder, H.F.H.M., Van Asch, T.W.J., 1988a. A stochastical approach to landslide determination in a forested area. Proceedings of the Vth International Symposium on Landslides, Lausanne, vol. 2. Balkema, Rotterdam, pp. 1207–1210.

Mulder, H.F.H.M., Van Asch, T.W.J., 1988b. On the nature and magnitude of variance of important geotechnical parameters. Proceedings of the Vth International Symposium on Landslides, Lausanne, vol. 1. Balkema, Rotterdam, pp. 239–243.

Olivry, J.-C., Hoorelbeck, J., 1989. Erosion des terres noires de la vallée du Buëch (Alpes-du-Sud). Cahier Orstom, Série Pédologie 25 (1–2), 95–110.

Oostwoud Wijdenes, D.J., Ergenzinger, P., 1998. Erosion and sediment transport on steep marly hillslopes, Draix, Haute-Provence, France: an experimental field study. Catena 33, 179–200.

Phan, T.S.H., 1993. Propriétés physiques et caractéristiques géotechniques des Terres Noires du Sud-Est de la France. PhD Thesis, Grenoble I University. 246 pp.

Phan, T.S.H., Antoine, A., 1994. Mineralogical and geotechnical characterization of the ''Black Lands'' of the South-East of France, having in view road applications. Proceedings of the VIIth International Congress of the Intenational Association of Engineering Geology, Lisboa, vol. 2. Balkema, Rotterdam, pp. 961–966.

Remaître, A., Maquaire, O., Pierre, S., 2002. Zones d'initiation et de contribution des laves torrentielles dans les bassins marneux. Exemple du torrent de Faucon (Bassin de Barcelonnette, Alpes-de-Haute-Provence). Géomorphologie: Relief, Processus, Environnement 2002-1, 71–84.

Rivière, A., 1977. Méthodes Granulométriques. Masson, Paris. 177 pp.

Serratrice, J.-F., 1978. Contribution à l'étude du comportement mécanique des marnes. PhD Thesis, Grenoble I University. 205 pp.

Serratrice, J.-F., 1995. Essais de laboratoire à haute pression sur des marnes, vol. 1. Colloquium Mondanum, Bruxelles, pp. 61–70.

Skempton, A.W., DeLory, F.A., 1957. Stability of natural slopes in London clay. Proceedings of the IVth International Conference on soil Mechanics and Foundation Engineering, Mexico, vol. 2. Mexican Society for Soil Mechanics, Mexico, pp. 378–381.

Tacnet, J.M., Gotteland, P., Bernard, A., Mathieu, G., Deymier, C., 2000. Mesures des caractéristiques géotechniques des sols grossiers. Applications aux sols de torrent. Proceedings of the Interpraevent Symposium, Villach, vol. 3. Tagungspublikation, Villach, pp. 307–319.

Tisot, J.-P., Houpert, R., 1980. Compactage des marnes raides fissurées. Cas des marnes du Keuper de Lorraine. Comptes-Rendus du Colloque International sur le Compactage, vol. 1. Ecole Nationale des Ponts et Chaussées, Paris, pp. 87–92.

Van Asch, T.W.J., 1997. The study of hydrological systems to understand changes in the temporal occurrence of landslides related to climatic changes. The temporal stability and activity of landslides in Europe with respect to climatic change (TESLEC). In: Dikau, R. et al. (Eds.), C.E.C. Environment Program, Contract EV5V-CT94-0454. EU, Brussels, pp. 69–86.

Van Asch, T.W.J., Buma, J., 1997. Modelling groundwater fluctuations and the frequency of movement of a landslide in the Terres Noires region of Barcelonnette, France. Earth Surface Processes and Landforms 22, 131–141.

Van Beek, L.P.H., Van Asch, T.W.J., 1996. The mobility characteristics of the La Valette landslide. Proceedings of the VIIth International Symposium on Landslides, Trondheim, vol. 2. Balkema, Rotterdam, pp. 1417–1421.